A CHARGE SEPARATION STUDY TO ENABLE THE DESIGN OF A COMPLETE MUON COOLING CHANNEL*

C. Yoshikawa#, C. Ankenbrandt, R. P. Johnson, Muons, Inc., Batavia, IL 60510, U.S.A.
Y. Derbenev, V. Morozov, JLAB, Newport News, VA 23606, U.S.A.
D. Neuffer, K. Yonehara, Fermilab, Batavia, IL 60510, U.S.A.

Abstract

The most promising designs for 6D muon cooling channels operate on a specific sign of electric charge. In particular, the Helical Cooling Channel (HCC) and Rectilinear RFOFO designs are the leading candidates to become the baseline 6D cooling channel in the Muon Accelerator Program (MAP). Time constraints prevented the design of a realistic charge separator, so a simplified study was performed to emulate the effects of charge separation on muons exiting the front end of a muon collider. The output of the study provides particle distributions that the competing designs will use as input into their cooling channels. We report here on the study of the charge separator that created the simulated particles.

INTRODUCTION

One of the most challenging components for a muon collider is the 6D cooling channel that must cool muons by six orders of magnitude in phase space before they decay (τ=2.2μs). The two most promising candidates are the Helical Cooling Channel [1,2] and Rectilinear RFOFO [3] designs. The Muon Accelerator Program (MAP) is a national effort headed at Fermilab that is charged with accessing the feasibility of building a muon collider and/or a neutrino factory based on a muon storage ring. A down-select competition between these contenders had been announced over the summer of 2013 with the expectation for each design to have results of simulations of all components in their channel by end of calendar 2013. Both concepts operate on a single sign of electric charge of the muon, but a charge separator had not been designed. The tight time constraint forbade the design of a realistic charge separator, so a study was performed to emulate the effects of a simplified charge separator on muons exiting the front end of a muon collider. The output of the study provides particle distributions that the competing designs will use as input into their cooling channels.

INITIAL STUDY

This study benefits from an earlier effort [4] that used bent solenoids to separate the opposite charges in the beam. Upon scrutiny of that study, we realized that it was possible to design a configuration that would separate the charges without the need to accelerate the muons above the momentum of 250 MeV/c expected from the front end of the system. A cartoon of the coil configurations that illustrate the basic layout of the charge separator is shown in Figure 1. There are two bent solenoids; the first "forward bend" (shown in white in Figure 1(a)) separates the charged beams vertically, while the second "reverse bend" (shown in red and blue in Figure 1) directs each beam back into the mid-plane. Each bend has three sectors: two "Norem matching" sectors [5] of half a Larmor oscillation length ($\lambda_L/2$) each and a mid-sector that has half the bending radius (and thus twice the vertical displacement angle) to adjust the vertical displacement at the end of the first bend. One of the beams will need to drift in a straight solenoid for a full λ_L in order to create separation between the two reverse bend sets of coils. For consistency with the earlier study, we chose the μ+ beam to traverse the longer path. Since there is no RF in the separator, the beam in the longer path is subject to larger longitudinal emittance growth, and that drives the performance of the charge separator. We will thus design to optimize the μ^+ beam and subsequently analyse the μ^- beam in the shorter channel.

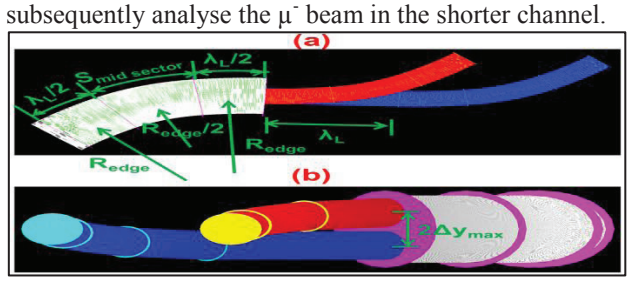

Figure 1: Cartoon of coil configuration illustrating the concept of a charge separator from a top view (a) and at the downstream end looking upstream (b).

A SIMPLIFIED CHARGE SEPARATOR

Designing a realistic charge separator will involve:

1. Dealing with fringe fields at the end of the forward bend and start of the two smaller solenoids.
2. Dealing with fringe fields between the two downstream solenoids.
3. Possibly tilting the coils in the downstream segments if the path difference introduced by the vertical displacement of the coils has a negative impact on performance.

The above complications and the time constraints motivated the need for a simulation setup that can extract the effects of a properly designed charge separator without having to design a realistic charge separator. Such a setup is illustrated in Figure 2 where the simple charge separator is introduced by way of two separate channels, one for each sign. Each channel incorporates large radii coils throughout both bends as well as in the

*Work supported in part by DOE STTR grant DE-SC0007634
#cary.yoshikawa@muonsinc.com

ISBN 978-3-95450-138-0

middle straight in the case of the longer μ+ channel. All coils are confined to lie in the mid-plane as would be done for the forward bend in a realistic charge separator. The coil configurations produce magnetic fields that are well understood and produce expected particle trajectories. Collimators are introduced in the sections downstream of the forward bend to mimic the effect of coil apertures in a realistic charge separator.

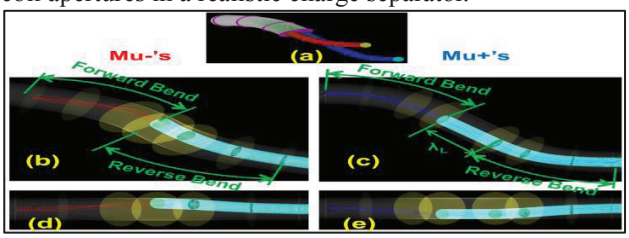

Figure 2: Association of a charge splitter coil concept in (a) to two separate simplified charge splitters (one for each sign) with transparent large radii coils. Yellow discs demarcate sectors. Oblique view of μ^-s in (b) and side view in (d) show vertical rise in forward bend and vertical drop in reverse bend. Oblique view of μ^+s in (c) and side view in (e) show vertical drop in forward bend and vertical rise in reverse bend.

OPTIMIZATION

The simple charge separator is utilized to optimize for maximum throughput and minimal longitudinal emittance growth, recalling there is no RF in the separator. As mentioned above, we will optimize for μ^+s which traverse the longer channel. Particles out of a 325 MHz version of the front end of a muon collider [6] were used as input, and since there is a roughly 20% loss of muons in the 4D cooler, we focused the optimization on particles exiting the phase rotator. Configurations considered in the optimization are given in Table 1, where each was designed to have the same vertical separation at the end of the first bend. Simulations were performed with G4beamline [7], and results of the optimization process are shown in Figure 3, where we have chosen the configuration with R_{edge}=6.32 m as the optimal based on transmission.

Table 1: Configurations in the Optimization

P=Pz	MeV/c	250						
B	T	2						
$\lambda_L=(2\pi P_z)/(B_\varphi c)$	m	2.62						
R_{edge}	m	3.21	4.25	5.28	6.32	7.36	8.39	9.43
α_{edge}(vert angle)	deg	7.4	5.6	4.5	3.8	3.2	2.8	2.5
$S_{mid\ sector}$	m	0	0.42	0.85	1.27	1.70	2.13	2.55
Δy_{max}	m	0.342						
$S_{Longer\ Channel}(\mu^+)$	m	7.86	8.71	9.56	10.41	11.26	12.11	12.96

LONGITUDINAL DISTORTION & ITS REMEDY

The μ^+s exiting the optimal charge separator configuration determined above will need to be caught into RF buckets immediately following the separator. Examination of the longitudinal phase space reveals distortion as shown in Fig. 4. Quantifying the particle losses and behaviour of ε_L in Fig. 5, a 9% loss and ε_L oscillation above the HCC acceptance is expected.

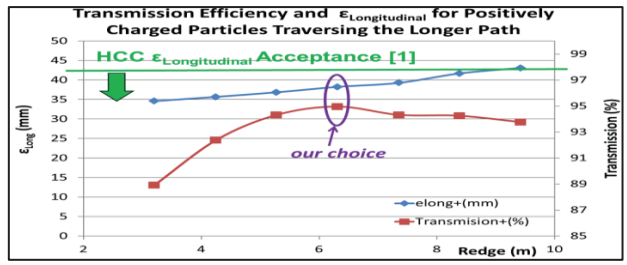

Figure 3: Results of optimization.

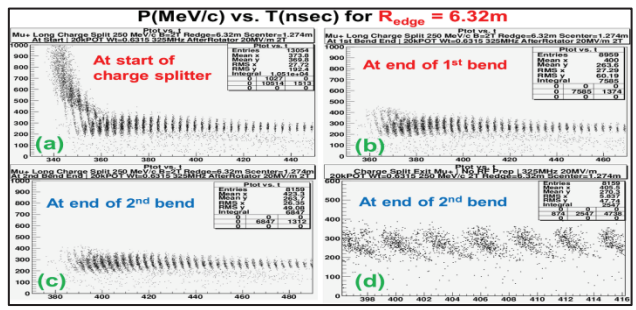

Figure 4: Longitudinal distortion at end of optimal configuration. P(MeV/c) vs. T(nsec) for μ+'s entering the charge separator are upright in (a) and begin to show some distortion at the end of the first bend in (b). Muons overlap neighboring bunches in (c), which is more easily seen in the zoomed-in view in (d).

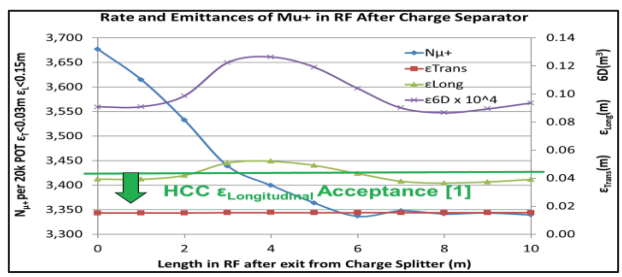

Figure 5: Rate and emittances of μ^+'s in RF after the charge separator.

A solution to counteract against this longitudinal distortion is to prepare the muon beam upstream of the charge separator as illustrated and explained in Figure 6, where RF gymnastics are applied to create a more upright ellipse in longitudinal phase space at the exit of the charge separator. Figure 7 shows the optimal configuration where particles exiting the phase rotator drift for 3 meters, followed by 4 m of RF (20 MV/m @ 325 MHz, same as upstream phase rotator) before traversing the charge separator and being caught and analysed in 10 m of RF of the same gradient and frequency. Figure 8 shows the longitudinal phase space of particles at the key locations described in Figure 6. While not perfectly upright, the particles that were subjected to the beam preparation in Figure 8(d) appear to have less distortion than those not having gone through the preparation in Figure 4(d).

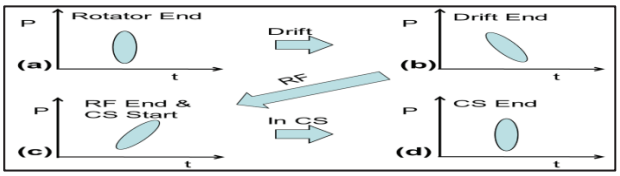

Figure 6: Longitudinal Phase Space Preparation Strategy. Longitudinal phase space of muons at the end of rotator in (a) are allowed to drift, resulting in (b) where RF is turned on to take advantage of the PvsT correlation. The rotated longitudinal phase space at end of the RF is shown in (c), which enters the charge separator and exits with an upright ellipse in (d).

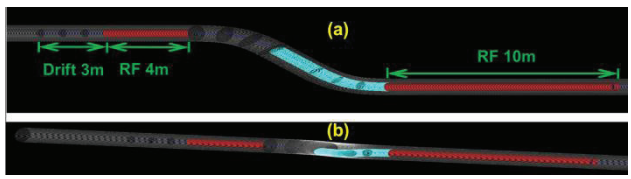

Figure 7: Oblique view in (a) of 3 m drift following phase rotator, followed by 4 m of RF (20 MV/m @ 325 MHz; same as rotator), followed by transit through the charge separator, followed by 10 m of RF to recapture the μ^+ beam. Side view is shown in (b).

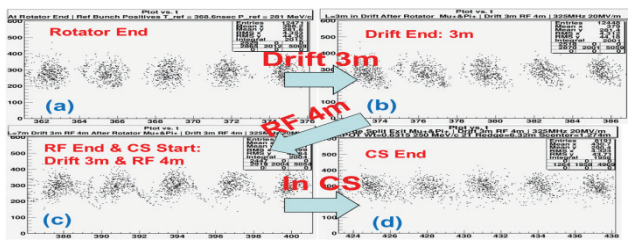

Figure 8: P(MeV/c) vs. T(nsec) for μ^+ through RF Preparation with 3 m of drift and 4 m of RF and traversed through the Charge Splitter. Panels a-d correspond to the same conditions as in Figure 6.

The improvement in rate of accepted muons and the reduction in the longitudinal emittance via the beam preparation are clearly seen in Figure **9** for μ^+s and Figure 10 for μ^-s. In the longer μ^+ channel, ε_L is lowered and remains within the HCC acceptance. The yield is also increased and remains flat in 10 m of RF, resulting in a net transmission increase of 14.6%. In the shorter μ^- channel, Figure 10 shows that while ε_L was within the HCC acceptance before the preparation, it is lowered further because of it. The increase in rate is not expected to be as dramatic, but is still significant at 10%. Final results are summarized in Table **2**.

SUMMARY

We presented a study to emulate the effects of a charge separator on muons exiting the front end of a muon collider to enable the design of a 6D cooling channel in absence of a realistic design of a charge separator. The output of this study provides particle distributions that the competing 6D cooling teams will use as input into their channels in the evaluation to be the baseline in MAP.

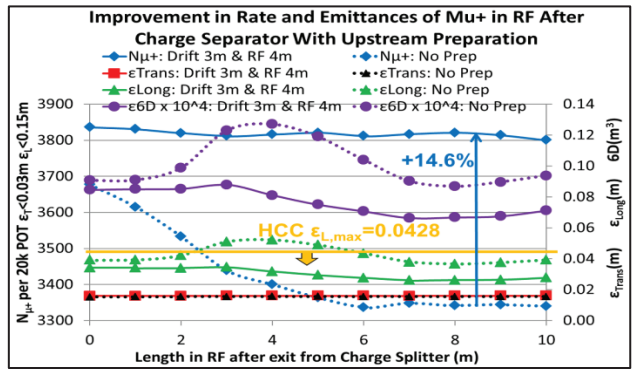

Figure 9: Improvement in Rate and Emittances of μ+'s in RF After Charge Separator with Upstream Preparation.

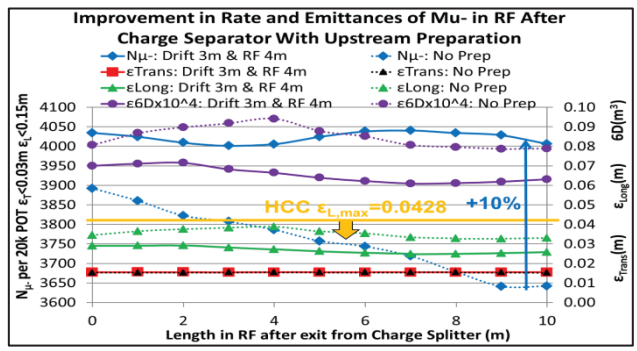

Figure 10: Improvement in Rate and Emittances of μ-'s in RF After Charge Separator with Upstream Preparation.

Table 2: Survival Rates and Emittances of Muons at 1 m Past a Charge Separator.

	ε_T		ε_L		ε_{6D}		$N_{survive}$	
units	mm-rad		mm		mm^3		per 20k POT	
Particle Species	μ^+	μ^-	μ^+	μ^-	μ^+	μ^-	μ^+	μ^-
At End of Rotator	15.66	15.54	30.06	27.71	7368	6690	4118	4221
R_{edge} = 6.32 m @ 1m Drift 3m; RF 4m	15.94	15.69	34.2	29.3	8519	7122	3831 (-7%)	4025 (-5%)
Acceptance of HCC	*20.4*		*42.8*		*12,900*			

REFERENCES

[1] K. Yonehara, R. P. Johnson, M. Neubauer, Y. S. Derbenev, "A helical cooling channel system for muon colliders", IPAC10, MOPD076, (2010).

[2] C. Yoshikawa, C. Ankenbrandt, R. P. Johnson, Y. S. Derbenev, V. Morozov, D. Neuffer, K. Yonehara "Complete Muon Cooling Channel Design and Simulations", IPAC13, TUPFI060 (2013).

[3] D. Stratakis et al., "A High-Performance Rectilinear FOFO Snake Channel for Muon Cooling", NA-PAC13, THPH012 (2013).

[4] R. Palmer and R. Fernow, "Charge Separation for Muon Collider Cooling", PAC11, MOP001 (2011).

[5] J. Norem, Phys. Rev. Spec. Top. – Acc. Beams 2, (1999) 054001.

[6] D. Neuffer and C. Yoshikawa, "Muon Capture for the Front End of a μ^+-μ^- Collider", PAC11, MOP030, (2011).

[7] G4beamline, T. Roberts, http://www.muonsinc.com

ISBN 978-3-95450-138-0